AGU PUBLICATIONS

JGR

Journal of Geophysical Research: Atmospheres

RESEARCH ARTICLE
10.1002/2015JD023082

Key Points:
- The DT and DB algorithms are inferior to SARA over Beijing-Tianjin-Hebei region
- SARA represents fine particles better than both DT and DB algorithms
- MYD04 DB C6 AOD retrievals are 3–4 times better than the DT C6 over Beijing

Correspondence to:
J. E. Nichol,
lsjanet@polyu.edu.hk

Citation:
Bilal, M., and J. E. Nichol (2015), Evaluation of MODIS aerosol retrieval algorithms over the Beijing-Tianjin-Hebei region during low to very high pollution events, *J. Geophys. Res. Atmos.*, *120*, 7941–7957, doi:10.1002/2015JD023082.

Received 7 JAN 2015
Accepted 13 JUL 2015
Accepted article online 16 JUN 2015
Published online 15 AUG 2015

Evaluation of MODIS aerosol retrieval algorithms over the Beijing-Tianjin-Hebei region during low to very high pollution events

Muhammad Bilal[1] and Janet E. Nichol[1]

[1]Department of Land Surveying and Geo-Informatics, The Hong Kong Polytechnic University, Hung Hom, Kowloon, Hong Kong

Abstract This study evaluates the performance of different MODerate resolution Imaging Spectroradiometer (MODIS) aerosol algorithms during fine particle pollution events over the Beijing-Tianjin-Hebei region using Aerosol Robotic Network aerosol optical depth (AOD). These algorithms include the Deep Blue (DB) Collection 5.1 (C5) and Collection 6 (C6) algorithms at 10 km resolution, the Dark Target (DT) C5 and C6 algorithms at 10 km, the DT C6 algorithm at 3 km, and the Simplified Aerosol Retrieval Algorithm (SARA) at 500 m, 3 km, and 10 km resolutions. The DB C6 retrievals have 34–39% less uncertainties, 2–3 times smaller root-mean-square error (RMSE), and 3–4 times smaller mean absolute error (MAE) than DB C5 retrievals. The DT C6 has 4–8% lower bias, 4–12% less overestimation, and smaller RMSE and MAE errors than DT C5. Due to underestimation of surface reflectance and the use of inappropriate aerosol schemes, 87–89% of the collocations of the DT C6 at 3 km fall above the expected error (EE), with overestimation of 64–79% which is 15–27% higher than that for the DT C6 at 10 km. The results suggest that the DT C6 at 3 km resolution is less reliable than that at 10 km. The SARA AOD has small RMSE and MAE errors with 90–96% of the collocations falling within the EE. Overall, the SARA showed 15–16% less uncertainty than the DB C6 (10 km), 69–72% less than the DT C6 (10 km), and 79–83% less than the DT C6 (3 km) retrievals.

1. Introduction

Satellite remote sensing has been used to quantify atmospheric aerosol concentrations associated with human health [*Pope et al.*, 2002], Earth's climate system [*Kaufman et al.*, 2002], and atmospheric visibility [*Cheung et al.*, 2005]. Aerosol optical properties such as aerosol optical depth (AOD) have been obtained from satellite sensors such as the Advanced Very High Resolution Radiometer [*Hauser et al.*, 2005; *Riffler et al.*, 2010], the Sea-viewing Wide Field of view Sensor [*Sayer et al.*, 2012], the Multiangle Imaging Spectroradiometer [*Kahn et al.*, 2005, 2010], the Total Ozone Mapping Spectroradiometer [*Torres et al.*, 2002], the Ozone Monitoring Instrument [*Torres et al.*, 2007], the MEdium Resolution Imaging Spectroradiometer [*Vidot et al.*, 2008], the Visible Infrared Imaging Radiometer Suite [*Jackson et al.*, 2013; *Liu et al.*, 2014], and the MODerate resolution Imaging Spectroradiometer (MODIS) [*Remer et al.*, 2005, 2008; *Levy et al.*, 2007b, 2010]. MODIS on board the Terra and Aqua satellites has been observing the Earth from space since 1999 and 2002, respectively, creating an extensive geophysical data set with 36 spectral channels, good temporal resolution of 1 to 2 days, and moderate spatial resolutions of 250 m, 500 m, and 1000 m. MODIS has been providing regular observations of AOD which have been used extensively in understanding the effects of anthropogenic aerosols at both local and global scales [*Kaufman et al.*, 2005; *Christopher et al.*, 2006]. The operational MODIS AOD product over land is based on two algorithms, namely, the Dark Target (DT) [*Kaufman et al.*, 1997; *Levy et al.*, 2007b, 2010] and Deep Blue (DB) [*Hsu et al.*, 2004, 2006] algorithms. The Collection 5.1 (C5) DT and DB algorithms have been extensively evaluated over land [*Remer et al.*, 2008; *Levy et al.*, 2010; *Hyer et al.*, 2011; *Shi et al.*, 2013].

In the recent years many Asian cities especially the Chinese capital, Beijing, have suffered severe deterioration in air quality with significant contributions from atmospheric particulates. For better understanding of the spatiotemporal behavior of these pollutants at city level, an effective and higher resolution satellite aerosol retrieval is required as MODIS DT and DB algorithms at 10 km resolution are unable to resolve city level aerosol features. Additionally, the DT algorithm works poorly over bright urban surfaces. Therefore, the MODIS aerosol team introduced a global DT AOD product at a nominal resolution of 3 km [*Remer et al.*, 2013] in the operational C6 AOD product. This is in addition to the DT [*Levy et al.*, 2013] and DB [*Hsu et al.*, 2013] AOD products at the standard 10 km resolution. The DT AOD product at 3 km is developed using a similar

Table 1. Summary of Data Sets Used in the Current Study for the Years 2012–2013

S/N	Instrument/Product	Parameter	Resolution		Purpose
			Original	Used	
1	AERONET	AOD	–	–	Input/validation
2	MYD02HKM	Radiance	500 m	500 m	Input
3	MYD03	Elevation and view angles	1000 m	500 m	Input
4	MYD09	Surface reflectance	500 m	500 m	Input
5	MYD04 C6	Cloud mask[a]	500 m	500 m	Input
		DT[b] and DB[c] AOD	10 km	10 km	Comparison
		Combined DT/DB[d] AOD	10 km	10 km	Comparison
6	MYD04 C5	DT[b] and DB[c] AOD	10 km	10 km	Comparison
7	MYD04_3 K C6	DT[b] AOD	3 km	3 km	Comparison

[a]Aerosol_Cldmask_Land_Ocean.
[b]Optical_Depth_Land_And_Ocean (QF = 3).
[c]Deep_Blue_Aerosol_Optical_Depth_550_Land (QF = 3).
[d]AOD_550_Dark_Target_Deep_Blue_Combined (QF = 3).

look-up table (LUT), surface estimation, and inversion methods as used in the existing DT C6 AOD product at 10 km, the only difference being in the selection of pixels in the retrieval window [*Remer et al.*, 2013]. Currently, the C6 product is available only for the Aqua satellite, and therefore, in the current study we only consider the Aqua-MODIS DT (3 km and 10 km) and DB (10 km) aerosol products over land.

Recently, a Simplified high resolution Aerosol Retrieval Algorithm (SARA) has been developed using Terra-MODIS data and validated over the complex urban and hilly terrain of Hong Kong using three different types of Sun photometers, including AErosol RObotic NETwork (AERONET), a Sky-radiometer, and Microtops II [*Bilal et al.*, 2013], as well as over the mixed urban surfaces of Beijing [*Bilal et al.*, 2014]. In this previous study [*Bilal et al.*, 2014] the SARA algorithm was evaluated over Beijing for its general performance compared with Terra-MODIS C5 DT algorithm at 10 km resolution and was found to perform well under a range of aerosol conditions including dust storms. The scope of the present study is much broader in evaluating additionally, three different Aqua-MODIS C6 AOD retrieval algorithms over the heavily urbanized and industrialized Beijing-Tianjin-Hebei region including very high pollution events dominated by fine particles. Therefore, this study evaluates the MODIS C5 and C6 DT AOD at 10 km, the DB C5 and C6 AOD at 10 km, the DT C6 AOD images at 3 km, and the SARA AOD at 500 m, 3 km, and 10 km resolutions during low to very high aerosols loading over the Beijing-Tianjin-Hebei region, all based on the Aqua-MODIS satellite over the years 2012–2013.

2. Data Sets and Methods

2.1. AERONET

The AErosol RObotic NETwork (AERONET) is a worldwide network of calibrated ground-based Sun photometers [*Holben et al.*, 1998, 2001] which provide cloud screened and quality assured spectral AOD [*Smirnov et al.*, 2000] in the range of 0.340 to 1.060 μm with low uncertainty (0.01–0.02) and high temporal resolution (every 15 min). In this study, data from four AERONET stations, Beijing, Beijing_RADI, Beijing_CAMS, and XiangHe, were obtained for the years 2012–2013 (Table 1). XiangHe AERONET is located in a suburban area of Tianjin, 70–80 km east of Beijing. These were cloud-screened and quality-controlled level 2.0 AOD measurements from the AERONET site "Beijing" (latitude: 39.977°, longitude: 116.381°) as well as level 1.5 AOD data (only cloud screened but not quality controlled) from the "Beijing_RADI" site (latitude: 40.005°, longitude: 116.379°), the "Beijing_CAMS" site (latitude: 39.933°, longitude: 116.317°), and the "XiangHe" site (latitude: 39.75360°, longitude: 116.96150°). Although Beijing levels 1.5 (only cloud screened) and 2.0 (cloud screened and quality assured) AOD data are highly correlated ($R^2 = 1$) with slope = 1 and offset = 0 for the years 2012–2013 as observed in this study, but it is always recommended to use level 2.0 data, if available, and results may be subject to large uncertainty if level 1.5 data are used.

2.2. Aqua MODIS Data

2.2.1. The MODIS DT (10 km and 3 km) and DB (10 km) Aerosol Retrieval Algorithms

For the development of the MODIS Dark Target (DT) aerosol retrieval algorithm over land at 10 km [*Remer et al.*, 2005, 2008; *Levy et al.*, 2007a, 2007b], reflectance at the top of the atmosphere (TOA) in the 2.11 μm

channel is calculated and corrected for gas absorption and dark-target pixels having reflectance between 0.01 and 0.25 are selected. Then for retrievals at 10 km and 3 km resolutions, pixels at 500 m resolution are organized into retrieval windows of 20×20 (400 pixels) and 6×6 (36 pixels), respectively. The 1.38 μm channel at 1000 m resolution is used to mask clouds, and snow/ice pixels including other bright surfaces are also masked, as the DT algorithm cannot retrieve aerosol information over these surfaces. The 0.66 μm channel at 250 m resolution is used to separate land from water pixels. The remaining pixels are aggregated at 500 m to create a collocated data set for further processing. The darkest 20% and brightest 50% of the remaining pixels of the 0.66 μm channel in the retrieval windows are deselected with, at most, 120 pixels (11 pixels) remaining in the retrieval window for 10 km (3 km) resolution to perform aerosol retrieval. This means that pixels at 3 km resolution might be retained that might be discarded at 10 km resolution, which makes the DT 3 km noisier than the 10 km product [*Levy et al*., 2013]. The DT algorithm at both 10 km and 3 km spatial resolutions is developed using similar aerosol inversion methods, LUT, and surface estimation based on the ratio of visible and shortwave infrared as a function of a vegetation index and scattering angle [*Levy et al*., 2013; *Remer et al*., 2013]. Modifications of C5 made for C6 are based on better assumptions of central wavelengths, Rayleigh optical depth and gases (H_2O, CO_2, and O_3), a revised range of solar zenith angle, normalized difference vegetation index $(NDVI)_{SWIR}$ dependence and Quality Assurance, and a revised and updated cloud mask for thin-cirrus and heavy-smoke detection [*Levy et al*., 2013]. The expected error (EE) over land of the DT algorithm at 10 km resolution is $\pm(0.05 + 15\%)$ and at 3 km resolution is $\pm(0.05 + 20\%)$ [*Levy et al*., 2013; *Remer et al*., 2013; *Munchak et al*., 2013; *Livingston et al*., 2014].

The MODIS Deep Blue (DB) algorithm was developed to retrieve AOD at 10 km resolution over bright desert surfaces utilizing deep blue wavelength, where the land surface reflectance is lower than for longer wavelengths [*Hsu et al*., 2004, 2006]. It retrieves aerosol information at 1 km resolution and then aggregates pixels into 10 km resolution, as opposed to the DT algorithm which first aggregates radiance into 10 km resolution and then performs the aerosol retrieval. For DB retrieval, pixels are masked and screened to eliminate clouds and snow/ice surfaces. For the remaining pixels, the surface reflectances are estimated for the 0.412, 0.47, and 0.65 μm channels using the minimum reflectivity method. Thus, AOD is retrieved at a nominal resolution of 1 km by finding the best match of TOA reflectances at 0.412, 0.47, and 0.65 μm channels with precalculated reflectances stored in the LUTs [*Hsu et al*., 2004, 2006]. The C6 contains the "second generation" DB algorithm [*Hsu et al*., 2013] which includes AOD retrieval for all dark and bright surfaces (except snow/ice), improved cloud screening and cirrus identification, an NDVI-dependent dynamic surface reflectance database, an improved aerosol model scheme for identification of dust particles, and revised Quality Assurance flags [*Hsu et al*., 2013]. The EE over land of the DB algorithm is $\pm(0.05 + 20\%)$ [*Hsu et al*., 2013; *Sayer et al*., 2013; *Shi et al*., 2013].

Because the DT algorithm [*Levy et al*., 2007a, 2007b] does not retrieve AOD over bright surfaces, including desert, the C6 includes a "best of" AOD product at 10 km resolution that combines both DT and DB (DT/DB) algorithms in the same image to retrieve aerosol over regions where DT algorithm does not retrieve [*Levy et al*., 2013]. In this study, the DT C5 and C6 AOD products at 10 km, the DB C5 and C6 AOD products at 10 km, the combined DT/DB C6 AOD at 10 km, and the DT C6 AOD product at 3 km are obtained from the MODIS Level 1 and Atmosphere Archive and Distribution System (http://ladsweb.nascom.nasa.gov) for the years 2012–2013, and only highest quality flag (QF = 3) AOD observations were utilized for analysis and comparison purposes.

2.2.2. The Simplified Aerosol Retrieval Algorithm

The Simplified Aerosol Retrieval Algorithm (SARA) requires top of the atmosphere (TOA) reflectance, surface reflectance, real viewing geometry, including solar and sensor zenith and azimuth angles, elevation, and aerosol information. As the SARA algorithm does not have prior knowledge of aerosol types over the region, this algorithm iterates a wide range of aerosol types and conditions $\omega_o = 0.30 - 1.0$ and $g = 0.0 - 1.0$ to retrieve AOD. In the current study, the SARA algorithm obtained TOA reflectance from MOD02HKM, viewing geometry and elevation from MOD03 geolocation product, surface reflectance from MOD09 product, and AOD information from a local AERONET station to compute the values of ω_o and g from the mentioned range for the day of retrieval. Similar to other aerosol retrieval algorithms, the SARA algorithm is dependent on accurate estimation of surface reflectance and can use surface reflectance estimated by different methods [*Hsu et al*., 2013; *Levy et al*., 2013; *Nazeer et al*., 2014]. The ready availability of the MOD09 surface reflectance product is the main reason for its use in the SARA algorithm. The success of the SARA algorithm is dependent

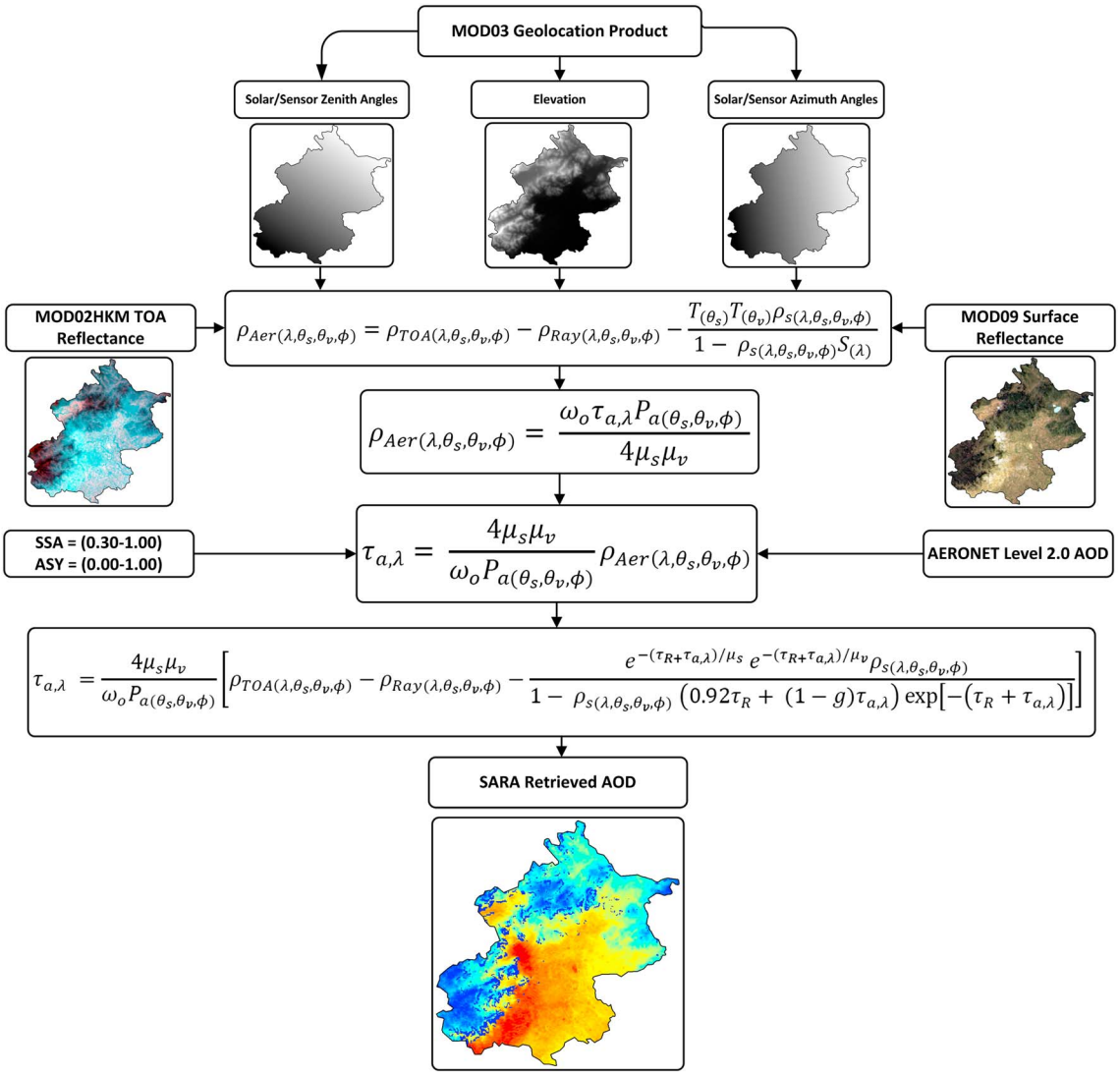

Figure 1. Block diagram of the Simplified Aerosol Retrieval Algorithm (SARA).

first on accurate estimation of surface reflectance (including aerosol correction) by MOD09 and second on the rigor of the SARA inversion for AOD. The algorithm performs aerosol retrieval over land for cloud-free images based on three assumptions: (i) the surface is Lambertian, (ii) the single scattering approximation is valid, and (iii) the single scattering albedo (ω_o) and asymmetric factor (g) remain spatially constant for a particular day [*Bilal et al.*, 2013]. The SARA algorithm can retrieve AOD directly for the green channel without the need to create a comprehensive look-up-table (LUT). The SARA-retrieved AOD was validated over Hong Kong [*Bilal et al.*, 2013], a coastal subtropical city with mixed aerosol types and moderate aerosol loadings, and Beijing [*Bilal et al.*, 2014], a city with sparse vegetation cover and under high aerosol loadings with greater influence of dust storms. The validation results of the SARA algorithm are very promising compared to the MODIS DT and other high-resolution MODIS aerosol retrieval algorithms [*Li et al.*, 2005, 2011; *Wong et al.*, 2010; *Wang et al.*, 2012]. In this study, the SARA AOD observations at 500 m, 3 km, and 10 km resolutions are retrieved for Aqua-MODIS swath products for the years 2012 and 2013 (Figure 1 and equation (1)) [*Bilal et al.*, 2013].

$$\tau_{a,\lambda} = \frac{4\mu_s\mu_v}{\omega_o P_{a(\theta_s,\theta_v,\phi)}} \left[\rho_{\mathrm{TOA}(\lambda,\theta_s,\theta_v,\phi)} - \rho_{\mathrm{Ray}(\lambda,\theta_s,\theta_v,\phi)} - \frac{e^{-\left(\tau_{R+}\tau_{a,\lambda}\right)/\mu_s} e^{-\left(\tau_{R+}\tau_{a,\lambda}\right)/\mu v} \rho_{s(\lambda,\theta_s\theta_v,\phi)}}{1 - \rho_{s(\lambda,\theta_s,\theta_v,\phi)} \left(0.92\tau_R + (1-g)\tau_{a,\lambda}\right) \exp\left[-\left(\tau_R + \tau_{a,\lambda}\right)\right]}\right], \quad (1)$$

where

$\tau_{a,\lambda}$ = aerosol optical depth (AOD),
τ_R = Rayleigh optical depth,
$\rho_{\mathrm{TOA}(\lambda,\theta_s,\theta_v,\phi)}$ = top of atmosphere (TOA) reflectance,
$\rho_{\mathrm{Ray}(\lambda,\theta_s,\theta_v,\phi)}$ = Rayleigh reflectance,
$\rho_{s(\lambda,\theta_s,\theta_v,\phi)}$ = surface reflectance,
μ_s = cosine of solar zenith angle,
μ_v = cosine of sensor zenith angle,
ω_o = single scattering albedo (SSA),
g = asymmetry parameter,
$P_{a(\theta_s,\theta_v,\phi)}$ = aerosol phase function.

2.3. Data Processing

The SARA AOD was retrieved at three different spatial resolutions, i.e., 500 m, 3 km, and 10 km resolutions using collocated data from Aqua-MODIS and level 2.0 AOD from the "Beijing" AERONET site. For SARA AOD at 3 km and 10 km resolutions, input data sets were resized into their respective required resolutions before applying the SARA algorithm to retrieve AOD. The retrieved AOD was then compared with AOD observations available at the same resolutions (3 km and 10 km) in the MYD04 C6 aerosol product. Retrievals were validated using collocated level 1.5 AOD from the other three AERONET sites, "Beijing_RADI", "Beijing_CAMS", and "XiangHe", located at a distance of around 3 km, 7 km, and 80 km, respectively, from the Beijing site. For comparison purposes, observations with only the highest quality flag (QF = 3) from the DT C5 and C6 AOD at 10 km, the DB C5 and C6 AOD at 10 km, the combined DT/DB C6 AOD at 10 km, and the DT C6 AOD at 3 km were obtained. To increase the number of statistical samples for validation, collocation was defined as the average of at least two AERONET AOD measurements between 12:00 and 14:00 local time and at least two pixels of MODIS AOD observations within a sampling window of 3×3 pixels (average of 9 pixels) centered on the AERONET site, i.e., average of 1.5 km × 1.5 km spatial region for the SARA AOD at 500 m, average of 9 km × 9 km spatial region for the MYD04_3 K and the SARA AOD at 3 km, and average of 30 km × 30 km spatial region for the MYD04 DT, the MYD04 DB, and SARA AOD at 10 km resolution. The total collocated data observations over both AERONET sites amount to 117 (C5) to 300 (C6) observations for DB at 10 km, 206 (C5) to 183 (C6) for DT at 10 km, 287 (C6) for combined DT/DB at 10 km, 174 (C6) for DT at 3 km, and 253 for SARA at 500 m, 3 km, and 10 km resolutions. Deming regression, an orthogonal regression technique, was used to estimate the slope and intercept of the data sets, and the uncertainty of each retrieval was evaluated using root-mean-square error (RMSE, equation (2)), mean absolute error (MAE, equation (3)), expected error over land (EE, equation (4)), and relative mean bias (RMB, equation (5)):

$$\mathrm{RMSE} = \sqrt{\frac{1}{n}\sum_{i=1}^{n}\left(\mathrm{AOD}_{(\mathrm{MODIS})i} - \mathrm{AOD}_{(\mathrm{AERONET})i}\right)^2} \tag{2}$$

$$\mathrm{MAE} = \frac{1}{n}\sum_{i=1}^{n}\left|\mathrm{AOD}_{(\mathrm{MODIS})i} - \mathrm{AOD}_{((\mathrm{AERONET}))i}\right| \tag{3}$$

$$\mathrm{EE} = \pm\left(0.05 + 0.15\mathrm{AOD}_{\mathrm{AERONET}}\right) \tag{4}$$

$$\mathrm{RMB} = \left(\overline{\mathrm{AOD}}_{(\mathrm{MODIS})}/\overline{\mathrm{AOD}}_{(\mathrm{AERONET})}\right) \ , \tag{5}$$

where RMB > 1.0 and RMB < 1.0 indicate the average overestimation and underestimation of the retrievals, respectively.

3. Results and Discussion

The MODIS DB C5 and C6 AOD at 10 km, the DT C5 and C6 AOD at 10 km, the combined DT/DB AOD at 10 km, the DT C6 AOD at 3 km, and the SARA-retrieved AOD at 500 m, 3 km, and 10 km are plotted against Beijing_RADI and Beijing_CAMS AERONET AOD measurements (Figures 2–6). In general, the quality of the MODIS aerosol retrievals depends on the accuracy of the surface reflectance and of the aerosol model, and overestimation/underestimation during clear and polluted days is normally caused by error in these two factors [*Chu et al.*, 2002; *Li et al.*, 2007; *He et al.*, 2010; *Xie et al.*, 2011]. It is reported by a previous study [*Xie et al.*, 2011] that the large intercept between MODIS DT algorithm and AERONET AOD at urban sites is

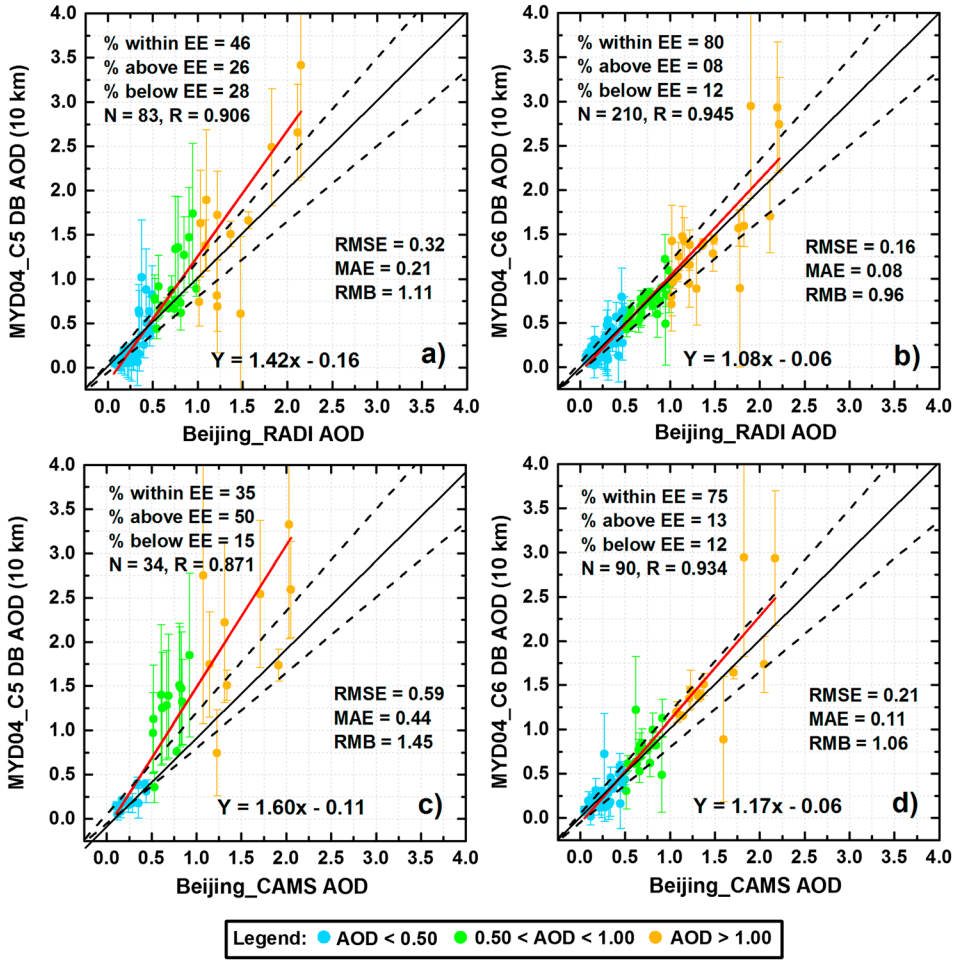

Figure 2. Validation of Aqua-MODIS DB (a and c) C5 and (b and d) C6 AOD observations at 10 km resolution against Beijing_RADI (Figures 2a and 2b) and Beijing_CAMS (Figures 2c and 2d) AERONET measurements for the years 2012–2013. The dashed lines = EE lines, black solid line = 1:1 line, and red solid line = regression line. Retrievals are selected using a sampling window of 3 × 3 pixels (average of 900 km^2 spatial region for the MYD04 DB AOD at 10 km) centered on the AERONET site.

due to a large uncertainty in the surface reflectance estimation. The validation of each algorithm is presented in the following sections, and the statistics are given in Table 2.

3.1. Validation of MODIS Deep Blue C5 and C6 Retrievals (10 km)

Figures 2a and 2c and 2b and 2d compare the C5 and C6 DB AOD observations at 10 km resolution respectively, with Beijing_RADI and Beijing_CAMS AERONET AOD measurements. In Figure 2, dashed lines represent the lower and upper boundaries of EE, and solid black and red lines are the 1:1 line and regression line, respectively. The DB collocations with AERONET for C6 (RADI = 210 and CAMS = 90) are almost 2.5 times those for C5 (RADI = 83 and CAMS = 34) at both AERONET sites, as C6 includes retrievals for all dark and bright surfaces (except snow/ice) [*Hsu et al.*, 2013]. The DB C5 underestimates during clearer days or during low aerosol loadings (AOD < 0.40) and overestimates during turbid days or during high aerosol loadings (AOD > 0.40) indicate overestimation of the surface reflectance and large error in aerosol model schemes, respectively. These errors lead to a large negative intercept (0.11–0.16) and a large slope (1.42–1.60) which introduces low-quality retrievals over both AERONET sites, with only 35–46% of the collocations falling within the EE. Similar results for Beijing are also reported by *Xie et al.* [2011]. Approximately 27–50% of the collocations falling above the EE cause overestimation of 11–45% (RMB = 1.11–1.45) compared with AERONET measurements. The modifications in the DB algorithm enable a better agreement between the C6 retrievals and AERONET AOD (R^2 = 0.873–0.892) than the C5 retrievals (R^2 = 0.759–0.821), with 2–2.8 times lower RMSE

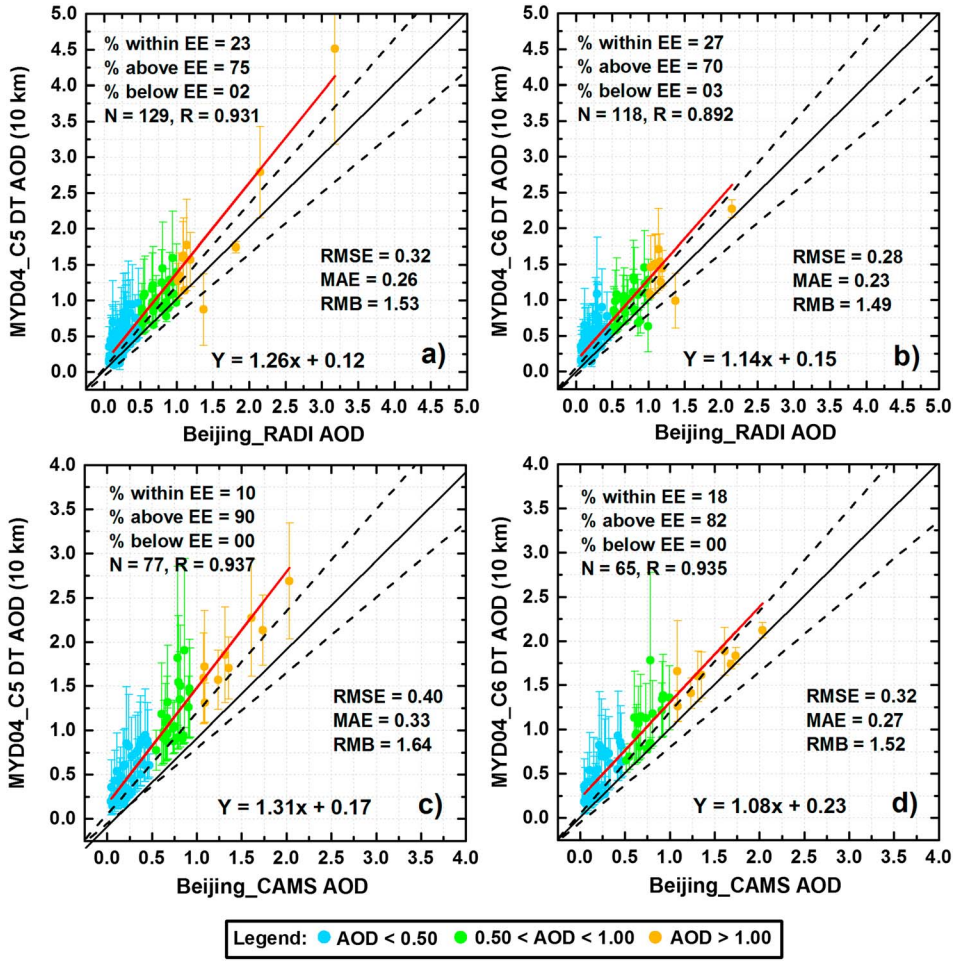

Figure 3. Validation of Aqua-MODIS DT (a and c) C5 and (b and d) C6 AOD observations at 10 km resolution against Beijing_RADI (Figures 3a and 3b) and Beijing_CAMS (Figures 3c and 3d) AERONET measurements for the years 2012–2013. The dashed lines = EE lines, black solid line = 1:1 line, and red solid line = regression line. Retrievals are selected using a sampling window of 3 × 3 pixels (average of 900 km^2 spatial region for the MYD04 DT AOD at 10 km) centered on the AERONET site.

and 2.6–4 times lower MAE errors. The numbers of collocations falling within the EE are increased by 75–80% which is 34–40% higher than that for DB C5. The NDVI-dependent dynamic surface reflectance estimation in the "second generation" DB algorithm appears to have improved the retrieval ability especially during low aerosol loadings which helps to reduce the intercept. Additionally, an improved aerosol model scheme helps to reduce the overestimation for $0.40 < AOD < 1.5$, although still the C6 retrievals are under/overestimated for very much polluted days when $AOD > 1.5$. These results indicate that the aerosol model scheme needs to be improved over Beijing for accurate retrieval of AOD levels above 1.5.

3.2. Validation of MODIS Dark Target C5 and C6 Retrievals (10 km)

Figure 3 shows the validation of DT C5 and C6 retrievals against Beijing_RADI and Beijing_CAMS AERONET AOD. The DT C5 overestimates AOD during clean and turbid days due to underestimation of the surface reflectance and the use of inappropriate aerosol optical properties in the LUT. Although C5 retrievals have a good correlation with AERONET AOD, but only 10–23% of the collocations fall within the EE, and a large number of retrievals have very large uncertainty, as 75–90% of the collocations fall above the EE leading to overestimation by 53–64% of the C5 retrievals.

The numbers of DT C6 collocations are fewer than those for DB C6 over both AERONET sites because DT C6 algorithm is unable to retrieve AOD over complex and bright urban surfaces, whereas DB C6 algorithm can retrieve AOD. The DT C6 retrievals have low RMSE and MAE errors, 4–8% less average overestimation, and

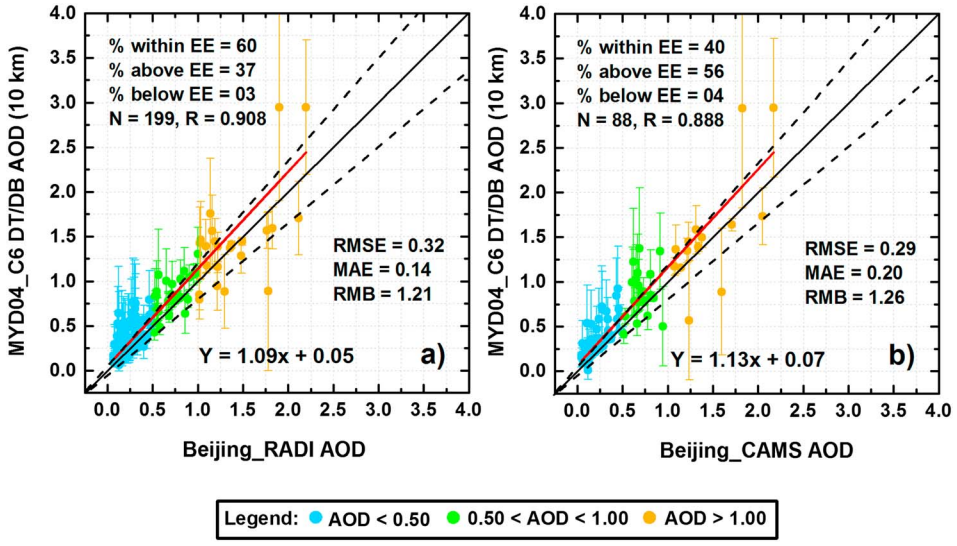

Figure 4. Validation of Aqua-MODIS combined DT/DB C6 AOD observations at 10 km resolution against (a) Beijing_RADI and (b) Beijing_CAMS AERONET measurements for the years 2012–2013. The dashed lines = EE lines, black solid line = 1:1 line, and red solid line = regression line. Retrievals are selected using a sampling window of 3 × 3 pixels (average of 900 km^2 spatial region for the MYD04 combined DT/DB AOD at 10 km) centered on the AERONET site.

4–8% lower retrieval uncertainty than the DT C5 retrievals. The AOD retrieved by C6 is better correlated with AERONET AOD during polluted days (AOD > 1.5) than the C5 AOD, but AOD is still highly overestimated during low to high aerosol loadings when AOD < 1.5 due to underestimation of the surface reflectance and large error in assumptions of the aerosol model used. These findings suggest that the MODIS DT C5 and C6 AOD observations are not suitable to use in further regional qualitative research applications due to large uncertainties. For more accurate AOD retrievals, improvements in the surface reflectance estimation as well as aerosol model schemes are required.

A larger number of collocations of the Terra-MODIS DT C5 [*Bilal et al.*, 2014] falling within the EE than that of the Aqua-MODIS DT C5 over Beijing for the same time period indicate a greater error in the Aqua-MODIS DT C5 than that in the Terra-MODIS DT C5. Since the retrieval algorithm is the same, this may be due to

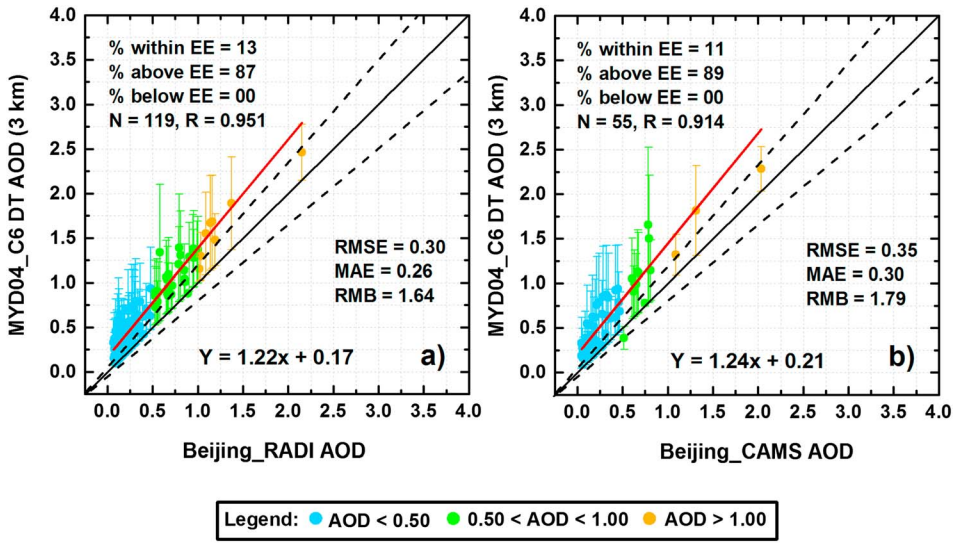

Figure 5. Validation of Aqua-MODIS DT C6 AOD observations at 3 km resolution against (a) Beijing_RADI and (b) Beijing_CAMS AERONET measurements for the years 2012–2013. The dashed lines = EE lines, black solid line = 1:1 line, and red solid line = regression line. Retrievals are selected using a sampling window of 3 × 3 pixels (average of 81 km^2 spatial region for the MYD04_3K AOD at 3 km) centered on the AERONET site.

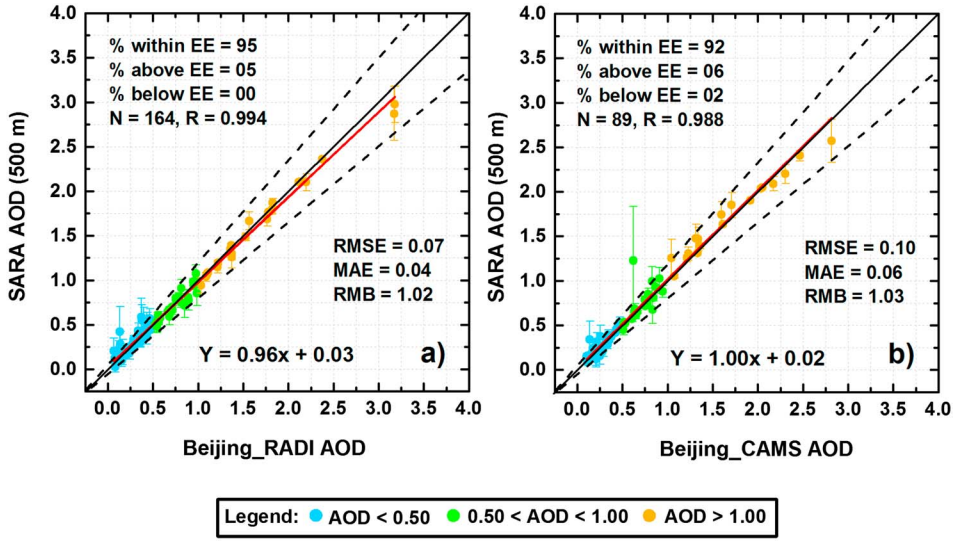

(6i)

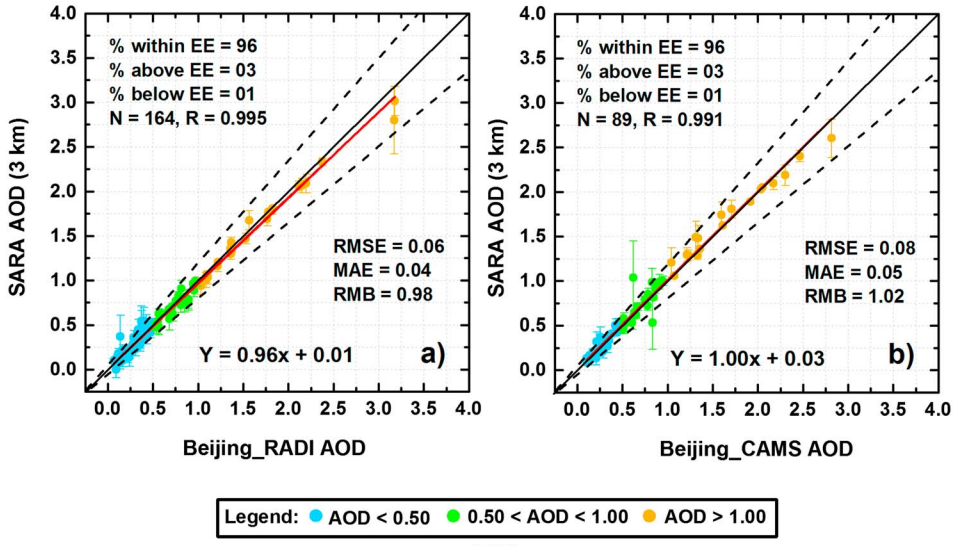

(6ii)

Figure 6. Validation of Aqua-SARA AOD observations at (i) 500 m, (ii) 3 km, and (iii) 10 km resolutions against (a) Beijing_RADI and (b) Beijing_CAMS AERONET measurements for the years 2012–2013. (iv): (a) Validation of Aqua-SARA AOD observations at 500 m with XiangHe AERONET AOD measurements; (b) comparison between Beijing and XiangHe AERONET AOD measurements. The dashed lines = EE lines, black solid line = 1:1 line, and red solid line = regression line. Retrievals are selected using s sampling window of 3 × 3 pixels (average of 2.25 km^2 spatial region for the SARA AOD at 500 m, average of 81 km^2 spatial region for SARA AOD at 3 km and average of 900 km^2 spatial region for SARA AOD at 10 km) centered on the AERONET site.

different aerosol types between mornings and afternoons. The Aqua-MODIS DT C5 also has only half the number of collocations falling within the EE, larger RMSE error, and shows 2 to 4 times the overestimation of Terra-MODIS DT C5 retrievals. Surprisingly, the Terra-MODIS DT C5 retrievals have less overestimation, smaller RMSE error, and a larger number of collocations falling within the EE than the Aqua-MODIS DT C6 retrievals. These results indicate that the Terra-MODIS DT C5 retrievals are significantly better than the Aqua-MODIS C5 and C6 retrievals over the urban surfaces of Beijing.

3.3. Validation of Combined MODIS DT/DB Retrievals (10 km)

Because DB C6 can retrieve AOD over both dark and bright surfaces, there is a greater contribution of DB to the combined DT/DB retrievals than of the DT C6. The greater contribution of the DB retrievals is

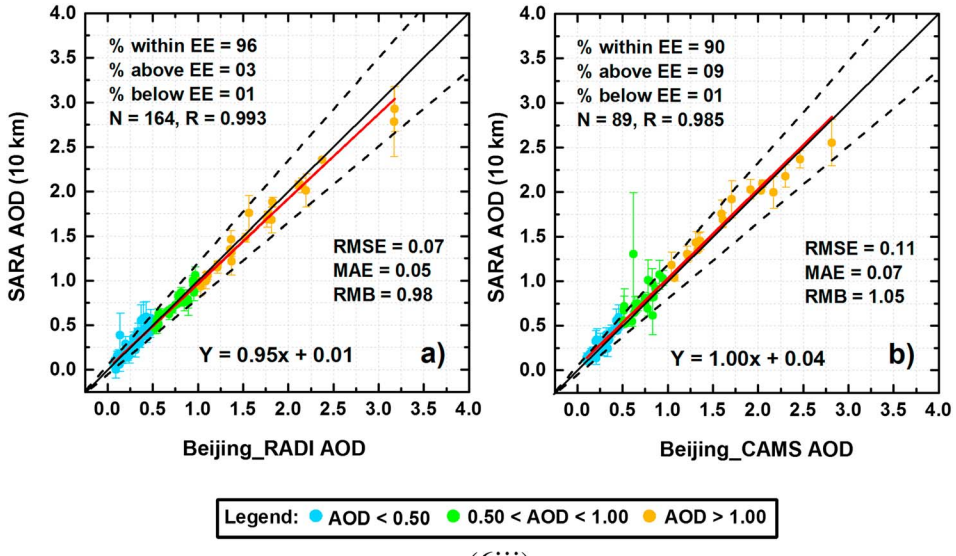

(6iii)

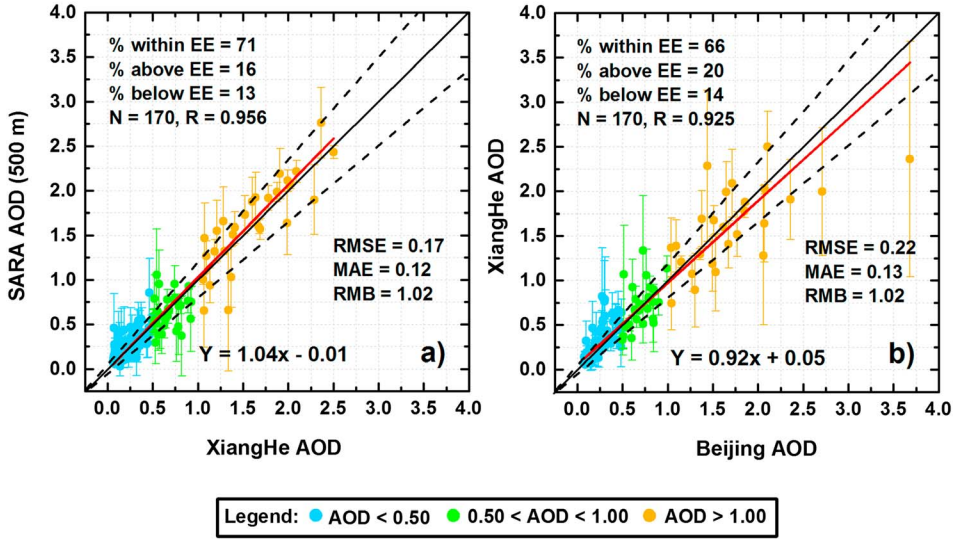

(6iv)

Figure 6. (continued)

accompanied by almost 2 times lower retrieval bias of DT/DB than DT C6, as 40–60% of the DT/DB collocations fall within the EE (Figure 4). The overestimation is reduced to half, with only half of the collocations above the EE. The large numbers of pixels with large uncertainty in the DT/DB retrievals are due to the greater contribution of the DT algorithm. During low-aerosol conditions, when AOD < 1.5, the DT/DB C6 is well retrieved compared with the DT C6 retrieval, and especially during very low aerosol loadings (AOD < 0.40), and better than the DT retrievals due to good approximation of surface reflectance in the "second generation" DB algorithm; this is also indicated by the very small intercept between DT/DB and AERONET measurements.

3.4. Validation of MODIS Dark Target C6 Retrievals (3 km)

Figure 5 shows that the number of collocations of MODIS DT C6 at 3 km is less than that at 10 km (Figure 3), which is similar to that reported by *Remer et al.* [2013] and *Munchak et al.* [2013]. We noted that similar to the DT algorithm at 10 km, the DT at 3 km overestimates over both AERONET sites during low

Table 2. Validation Summary of DT (C5 and C6), DB (C5 and C6), Combined DT/DB (C6), DT_3 K (C6), and SARA (500 m, 3 km, and 10 km) Collocations

	N	Mean	StDev	RMSE	% within EE	% Above EE	% Below EE
DB-Beijing_RADI Collocations (10 km)							
AERONET	83	0.53	0.47				
DB C5		0.58	0.67	0.32	46	27	28
AERONET	210	0.44	0.45				
DB C6		0.42	0.48	0.16	80	8	12
DB-Beijing_CAMS Collocations (10 km)							
AERONET	34	0.76	0.55				
DB C5		1.11	0.89	0.59	35	50	15
AERONET	90	0.52	0.48				
DB C6		0.55	0.57	0.21	75	13	12
DT-Beijing_RADI Collocations (10 km)							
AERONET	129	0.46	0.44				
DT C5		0.70	0.55	0.32	23	75	2
AERONET	118	0.42	0.36				
DT C6		0.63	0.42	0.28	27	70	3
DT-Beijing_CAMS Collocations (10 km)							
AERONET	77	0.52	0.42				
DT C5		0.85	56	0.40	10	90	0
AERONET	65	0.52	0.47				
DT C6		0.79	0.51	0.32	18	82	0
DT/DB-Beijing_RADI Collocations (10 km)							
AERONET	199	0.43	0.43				
DT/DB C6		0.52	0.47	0.32	60	37	3
DT/DB-Beijing_CAMS Collocations (10 km)							
AERONET	88	0.53	0.49				
DT/DB C6		0.66	0.55	0.29	40	56	4
DT_3K-Beijing_RADI Collocations (3 km)							
AERONET	119	0.40	0.36				
DT 3 K C6		0.66	0.44	0.30	13	87	0
DT_3K-Beijing_CAMS Collocations (3 km)							
AERONET	55	0.37	0.36				
DT 3 K C6		0.67	0.45	0.35	11	89	0
SARA-Beijing_RADI Collocations (500 m, 3 km and 10 km)							
AERONET	164	0.52	0.57				
SARA (500 m)		0.53	0.55	0.07	95	5	0
SARA (3 km)		0.51	0.55	0.06	96	3	1
SARA (10 km)		0.51	0.55	0.07	96	3	1
SARA-Beijing_CAMS Collocations (500 m, 3 km and 10 km)							
AERONET	89	0.65	0.62				
SARA (500 m)		0.67	0.62	0.10	92	6	2
SARA (3 km)		0.66	0.62	0.08	96	3	1
SARA (10 km)		0.69	0.62	0.11	90	9	1

and high aerosol loadings, due to a large bias in both surface reflectance estimation and assumption of aerosol models, and as a result 11–13% and 87–89% of the 3 km collocations fall within and above the EE, respectively, indicating almost 2 times greater retrieval uncertainty and leading to overestimation of 64–79% which is 15–27% greater than the DT at 10 km. The overestimation of AOD retrievals over Beijing is due to underestimation of the surface reflectance in the visible channels, as incorrect estimation of the surface reflectance is considered the primary source of error in the DT product at 3 km [*Munchak et al.*, 2013]. This effect appears more at 3 km than at 10 km, because in the latter most of the bright urban surfaces in the DT retrieval box are discarded during the pixel selection process in the 0.66 μm channel [*Munchak et al.*, 2013]. These results indicate that the new MODIS DT C6 product at 3 km is not promising at regional scale and is less reliable than DT C6 at 10 km resolution over the mixed urban surfaces of Beijing.

3.5. Validation of SARA Retrievals (500 m, 3 km, and 10 km)

AOD observations at 500 m (Figure 6i), 3 km (Figure 6ii), and 10 km (Figure 6iii) resolutions are retrieved using the SARA algorithm and plotted against Beijing_RADI and Beijing_CAMS AERONET measurements. The SARA retrievals are highly correlated ($R^2 \sim 0.970–0.990$) with the AERONET measurements, with a slope close to 1 (slope ~ 0.95–1.00), a very small positive offset (intercept ~ 0.01–0.04), and small RMSE (~0.07–0.11) and MAE (~0.04–0.0.07). The SARA AOD is also well retrieved during low to high aerosol loadings and much polluted days (AOD > 1.5) as 90–96% of the collocations fall within the EE, which indicates very low bias in the SARA retrievals. Only 5–6% of the collocations fall above the EE, meaning that the SARA retrievals show negligible overestimation (only 2–3%) over the urban surfaces of Beijing. Additionally, unlike DT C5, the SARA algorithm has good retrievals and almost the same low uncertainty for Terra-MODIS [*Bilal et al*., 2014] as for Aqua-MODIS over Beijing. The uncertainty in the SARA retrievals is mainly due to MOD09 as surface reflectance along with TOA reflectance are used to compute ω_o and g. Overall, the SARA collocations are highly correlated with AERONET during both low and high aerosol loadings, with 15–16% lower retrieval bias than the DB C6 at 10 km resolution, 69–72% better than the DT C6 at 10 km, 35–52% better than the combined DT/DB C6 at 10 km, and 79–83% better than the DT C6 at 3 km resolution.

As discussed in section 2.2.2, AOD measurements from Beijing AERONET are used in the SARA algorithm to retrieve AOD with the assumption that "ω_o" and "g" are constant over the region for the day of retrieval. The SARA-retrieved AOD observations are validated using XiangHe AERONET which is located in a suburban area of Tianjin 70–80 km east of Beijing. The validation result (Figure 6iv-a) shows that 71% of the SARA retrievals fall within the EE, indicating that more than 60% of the days have similar aerosol conditions between XiangHe and Beijing which favors the assumptions that ω_o and g do not vary on most days. An examination of the relationship between the AOD values from "Beijing" and "XiangHe" AERONET stations is performed (Figure 6iv-b) to demonstrate the difference in aerosol types between the urban area of Beijing and the suburban area of Tianjin using the EE over land as an indicator. Figure 6iv-b shows that 66% of the AOD measurements from XiangHe AERONET fall within the EE, indicating that SARA's uncertainty in retrieving AOD at XiangHe (71% within EE) is similar to the uncertainty in XiangHe AERONET AOD due to differences in aerosol conditions alone between Beijing and XiangHe. These results suggest that uncertainty in the SARA retrievals may increase as the SARA algorithm is used at greater distances (70–80 km) from the AERONET station used for determining the ω_o and g.

To understand errors in the SARA retrievals, a sensitivity analysis of the SARA AOD at 500 m resolution is performed by increasing/decreasing by 5% the value of aerosol phase function ($P_a \pm 0.05P_a$). The new SARA-retrieved AOD observations are validated with Beijing_RADI and Beijing_CAMS AERONET AOD data and then compared with the original results (Figure 6i). This showed that errors are increased 4% to 8% by decreasing and increasing the 5% value of P_a, respectively, over both AERONET sites. These results confirm that P_a is not introducing large errors, and the SARA retrievals are acceptable over the region as 84–91% of the retrievals fall within the EE. Sensitivity analysis for other parameters was conducted in our former study [*Bilal et al*., 2013].

3.6. High Aerosol Loading Over the Beijing-Tianjin-Hebei Region

China has suffered from serious air pollution problems due to high aerosol loadings for many years, the major sources being vehicle exhaust emissions, coal burning, and dust storms. On several occasions in 2013, skies over the Beijing-Tianjin-Hebei region darkened due to the presence of heavy haze, smog, and dust particles in the atmosphere. To identify the best method for monitoring air quality in this region where aerosol levels are frequently higher than in most other regions, very high aerosol loading events (AOD > 3.0) on 28 September 2013, 5 October 2013, and 9 October 2013 are selected for comparison among the DB (10 km), DT (10 km, and 3 km) and SARA (500 m) algorithms (Figure 7). The Aqua-MODIS band 4 (550 nm) pseudo color image (Figures 7i–7iii)) shows the Beijing-Tianjin-Hebei region under the influence of fine particles with low to high concentrations. The dominance of fine particles is confirmed from AERONET level 2 inversion data which give the size distribution. XiangHe AERONET also recorded high AOD during these very high pollution events and is used for validation of the MODIS AOD retrievals. The cloud mask at 500 m resolution was obtained from the Scientific Data Set "Aerosol_Cldmask_Land_Ocean" of the MYD04 C6 aerosol product to highlight missing pixels (grey) and cloud contamination (white). The

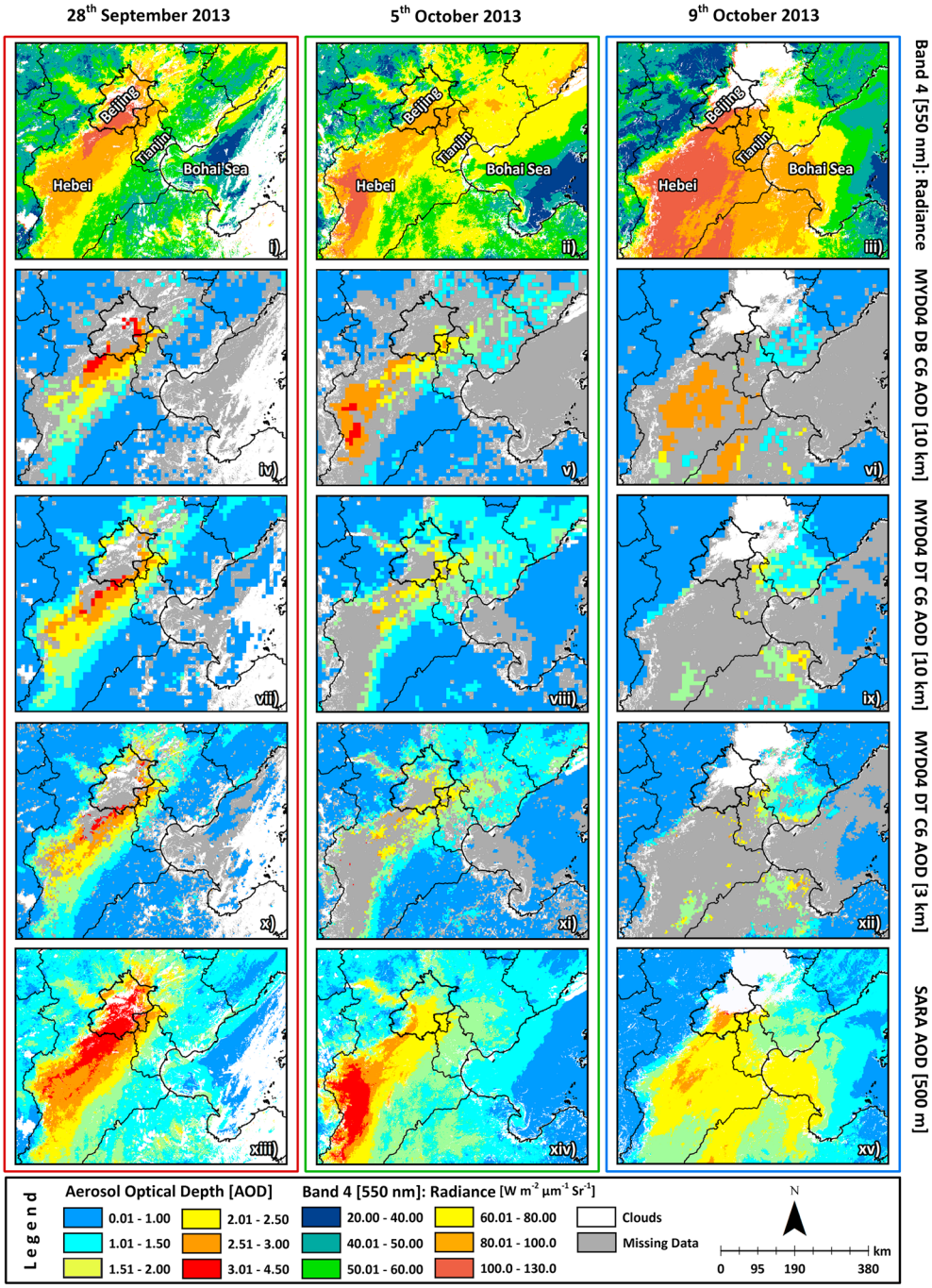

Figure 7. High aerosol concentrations over the Beijing-Tianjin-Hebei region on 28 September 2013, 5 October 2013, and 9 October 2013: (i–iii) Band 1 pseudo color image, (iv–vi) MYD04 DB C6 AOD (10 km), (vii–ix) MYD04 DT C6 (10 km), (x–xii) MYD04 DT C6 AOD (3 km), and (xiii–xv) SARA AOD (500 m).

MYD04 cloud mask appears to be biased over the coastal region of the Bohai Sea where it is unable to distinguish between clouds and coastal sediments, and has flagged pixels over the coastal boundary as cloud, which can be seen in Figure 7.

Figures 7iv–7vi show the spatial distribution of the DB C6 AOD retrieved over the Beijing-Tianjin-Hebei region, where clouds are white and grey color represents missing pixels. The DB C6 retrieved AOD over the XiangHe AERONET site falls within the EE on 28 September 2013, whereas the DB algorithm overestimates and has missing pixels on both 5 October 2013 and 9 October 2013 (Table 3). The DB C6 algorithm is unable

Table 3. Validation of MODIS Aerosol Algorithms Using AERONET AOD During High Concentrations of Fine Particles Over Beijing-Tianjin-Hebei Region

	AERONET	AOD Algorithms				Expected Error	
Pollution Events (2013)	XiangHe	DB (10 km)	DT (10 km)	DT (3 km)	SARA (500)	Lower Limit	Upper Limit
28 Sep	2.36	2.59	2.57	2.59	2.76	1.96	2.77
5 Oct	1.91	2.38	2.23	2.30	2.19	1.57	2.24
9 Oct	2.00	Missing	Missing	Missing	2.11	1.65	2.34

to depict fine pollutants during high aerosol-loading events at regional level and has a large number of missing pixels over the region. The DT algorithm at both 10 km (Figures 7vii–7ix) and 3 km (Figures 7x–7xii) is unable to retrieve AOD over the region with high aerosol concentrations and shows missing pixels. These missing pixels are not due to cloud cover, as this is a cloud-free area (Figure 7), and the omission is likely due to either deselection of the pixels in the 0.66 μm channel where the DT algorithm discards 20% of the darkest and 50% of the brightest pixels, or unavailability of the input data for DT retrieval. The DT AOD at 10 km is more accurate than that at 3 km, falling within the EE (Table 3). However, both the DB and the DT retrievals are underestimated over the western regions of Beijing and Bohai Sea on 28 September 2013 (Figure 7i) and 5 October 2013 (Figure 7ii). The SARA algorithm performed well for these high pollution events and clearly highlights the areas of low and high aerosol concentrations with high spatial detail (Figures 7xiii–7xv). The SARA-retrieved AOD over the XiangHe AERONET site falls within the EE, indicating high confidence in the SARA retrieval during the fine particle pollution events with AOD > 3.0. Also, the SARA AOD is well retrieved over the western regions of Beijing and Bohai Sea where the DB and the DT retrievals are underestimated.

Figure 7 shows that the SARA algorithm gives a complete and detailed spatial coverage at finer spatial resolution (500 m) with no missing data and is better able to retrieve AOD during severe pollution when fine particles are dominant. This supplements our previous study over Beijing [*Bilal et al*., 2014], where the SARA algorithm was better able to retrieve AOD during an extreme dust event (17 April 2006) than the MODIS DT and DB algorithms. From these studies we conclude that the SARA algorithm is much more efficient than both the MODIS DT and DB algorithms to retrieve AOD over the Beijing-Tianjin-Hebei region in the presence of either fine or coarse aerosol particle loadings and is robust over a wide range of surface types and aerosol conditions.

3.7. Spatial Comparison Between SARA and Aqua-MODIS L2 Products

In order to test the effectiveness of SARA at locations distant from the AERONET stations used for obtaining ω_o and g, the DB retrievals are treated as the reference data set for comparison with DT and SARA AOD observations over a large region including 50 sites in the Beijing-Tianjin-Hebei region for the years 2012–2013. This is because as observed in section 3.1, the DB AOD retrievals show much lower uncertainty

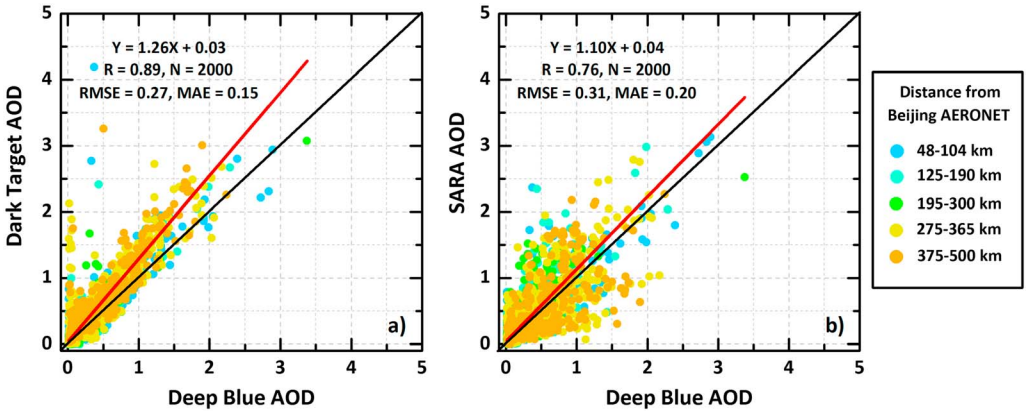

Figure 8. Spatial comparison between (a) DT and DB AOD, and between (b) SARA and DB AOD over Beijing-Tianjin-Hebei region for the years 2012–2013. Colors represent distance from Beijing AERONET site, where sites with blue color are close (minimum distance = 48 km) to the AERONET and sites with orange color are far from AERONET (maximum distance = 500 km).

Table 4. Spatial Statistics of SARA and Aqua-MODIS L2 Products Over Beijing-Tianjin-Hebei Region for 2012–2013

Algorithm	*N*	*R*	Slope	Intercept	Mean	StDev	RMSE	MAE	Distance From AERONET
Deep Blue AOD Versus Dark Target AOD									
DB	466	0.86	1.18	0.01	0.33	0.42	0.27	0.11	48–104 km
DT					0.40	0.50			
DB	375	0.92	1.27	0.02	0.25	0.32	0.17	0.10	125–190 km
DT					0.34	0.40			
DB	323	0.90	1.12	0.02	0.21	0.29	0.15	0.08	195–300 km
DT					0.26	0.32			
DB	508	0.87	1.25	0.09	0.43	0.44	0.34	0.22	275–365 km
DT					0.62	0.55			
DB	348	0.89	1.29	0.06	0.48	0.43	0.33	0.22	375–500 km
DT					0.69	0.56			
Deep Blue AOD Versus SARA AOD									
DB	466	0.86	1.05	0.02	0.33	0.42	0.23	0.13	48–104 km
SARA					0.37	0.44			
DB	375	0.77	1.31	0.04	0.25	0.32	0.29	0.19	125–190 km
SARA					0.38	0.42			
DB	323	0.77	1.26	0.11	0.21	0.29	0.28	0.19	195–300 km
SARA					0.38	0.36			
DB	508	0.73	1.07	0.01	0.43	0.44	0.34	0.23	275–365 km
SARA					0.47	0.48			
DB	348	0.68	1.09	−0.02	0.48	0.43	0.36	0.25	375–500 km
SARA					0.51	0.47			

than the DT retrievals, although they are not 100% accurate, showing 22.5% mean uncertainty over Beijing AERONET sites. The DB retrieval uncertainty is ignored in the comparison analysis (Figure 8).

Figure 8b shows that SARA AOD correlates well spatially ($R = 0.76$) with the DB AOD but is slightly lower than the DT AOD (Figure 8a, $R = 0.89$), although both have similar RMSE and MAE (Table 4). The SARA AOD retrievals are more scattered than those of DT, and retrieval errors in the SARA algorithm are due to the assumption that single scattering albedo (SSA) and g are spatially constant over the region. For low DB AOD, very high values of DT AOD are observed, and overall the DT retrievals are overestimated which leads to higher slope (= 1.26) than the SARA retrievals (slope = 1.10).

Table 4 shows that the SARA retrievals achieved good correlation for all the spatial sites, with higher correlation for the sites close to the AERONET sites and lower correlation for more distant sites. Similarly, RMSE and MAE increase with distance from the AERONET sites. However, a similar trend is observed for the DT retrievals, which show an even higher mean AOD difference (0.40) than the SARA retrievals (mean AOD difference = 0.07) for the distant sites 29–50. The errors in the SARA retrievals are due to the use of constant values of SSA and g for the day of retrieval, but overall the SARA retrievals are better in the sense of higher spatial resolution and lower uncertainties over the AERONET sites compared to the Aqua-MODIS L2 retrievals.

4. Conclusion

The objective of this study was to evaluate the Aqua-MODIS AOD retrieval product including Deep Blue C5 and C6 AOD at 10 km, Dark Target C5 and C6 AOD at 10 km, the combined DB/DT AOD at 10 km, DT C6 AOD at 10 km, and SARA AOD at 500 m, 3 km, and 10 km resolutions using measurements from two AERONET stations over the mixed surfaces of Beijing. The results showed that the DB C5 AOD algorithm overestimated during low to high aerosol loadings due to large bias in the surface reflectance estimation and aerosol model used. However, the "second-generation" DB C6 was able to reduce these errors and retrieved AOD well compared with AERONET measurements during both clear and turbid days and has lower retrieval uncertainty than DB C5, indicating significant improvements in the DB C6 over the C5 algorithm. The DB C6 algorithm still overestimated during very polluted days when AOD > 1.5, and improvements are required for accurate AOD retrieval during these days. Significant improvements in the DT C6 were not evident, as the retrieval quality of the DT C6 algorithm appeared similar to DT C5. The DT C5 and C6 AOD overestimated during low to high aerosol loadings (AOD < 1.5) due to large error in the surface reflectance

and aerosol schemes, but DT C6 retrieved better during very polluted days (AOD > 1.5) than DT C5. The combined DT/DB C6 AOD appeared superior to DT C6 AOD due to the greater contribution of DB retrievals. The DT C6 AOD at 3 km is greatly overestimated and has very poor retrieval quality compared to that at 10 km. The results also showed that the SARA AOD retrievals are much more accurate than the DT and DB retrievals over AERONET sites for low to high aerosol loadings, as well as on highly polluted days. Overall, the results demonstrate that the SARA algorithm is much more efficient and robust than both the DT and DB algorithms over Beijing-Tianjin-Hebei region, as SARA is region-specific, whereas DT and DB are global algorithms. It can perform well during high pollution events dominated by fine particles (AOD > 3.0) and is able to depict detailed spatial variations in aerosol patterns. A regional map of the AOD gradient from the SARA algorithm can be useful in constraining model/forecasts for surface air quality.

Acknowledgments

The data for this paper are available at Level 1 and Atmosphere Archive and Distribution System (http://ladsweb.nascom.nasa.gov) and AERONET Web (http://aeronet.gsfc.nasa.gov). We would like to thank the principal investigators of the four AERONET stations: Beijing, Beijing_RADI, Beijing_CAMS, and XiangHe, and also Brent Holben for helping with the AERONET stations. We are thankful to Devin White (Oak Ridge National Laboratory) for MODIS Conversion Tool Kit (MCTK), the reviewers for their valuable suggestions and comments that have greatly improved the quality of the paper, and the help of Max P. Bleiweiss (New Mexico State University) in the revision of this manuscript. Grant PolyU5225/13E from the Hong Kong Research Grants Council sponsored this research.

References

Bilal, M., J. E. Nichol, M. P. Bleiweiss, and D. Dubois (2013), A Simplified high resolution MODIS Aerosol Retrieval Algorithm (SARA) for use over mixed surfaces, *Remote Sens. Environ.*, *136*, 135–145, doi:10.1016/j.rse.2013.04.014.

Bilal, M., J. E. Nichol, and P. W. Chan (2014), Validation and accuracy assessment of a Simplified Aerosol Retrieval Algorithm (SARA) over Beijing under low and high aerosol loadings and dust storms, *Remote Sens. Environ.*, *153*, 50–60, doi:10.1016/j.rse.2014.07.015.

Cheung, H.-C., T. Wang, K. Baumann, and H. Guo (2005), Influence of regional pollution outflow on the concentrations of fine particulate matter and visibility in the coastal area of southern China, *Atmos. Environ.*, *39*(34), 6463–6474, doi:10.1016/j.atmosenv.2005.07.033.

Christopher, S. A., J. Zhang, Y. J. Kaufman, and L. A. Remer (2006), Satellite-based assessment of top of atmosphere anthropogenic aerosol radiative forcing over cloud-free oceans, *Geophys. Res. Lett.*, *33*, L15816, doi:10.1029/2005GL025535.

Chu, D. A., Y. J. Kaufman, C. Ichoku, L. A. Remer, D. Tanré, and B. N. Holben (2002), Validation of MODIS aerosol optical depth retrieval over land, *Geophys. Res. Lett.*, *29*(12), 8007, doi:10.1029/2001GL013205.

Hauser, A., D. Oesch, N. Foppa, and S. Wunderle (2005), NOAA AVHRR derived aerosol optical depth over land, *J. Geophys. Res.*, *110*, D08204, doi:10.1029/2004JD005439.

He, Q., C. Li, X. Tang, H. Li, F. Geng, and Y. Wu (2010), Validation of MODIS derived aerosol optical depth over the Yangtze River Delta in China, *Remote Sens. Environ.*, *114*(8), 1649–1661, doi:10.1016/j.rse.2010.02.015.

Holben, B. N., et al. (1998), AERONET—A federated instrument network and data archive for aerosol characterization, *Remote Sens. Environ.*, *66*(1), 1–16, doi:10.1016/S0034-4257(98)00031-5.

Holben, N., et al. (2001), An emerging ground-based aerosol climatology: Aerosol optical depth from AERONET, *J. Geophys. Res.*, *106*(DII), 12,067–12,097, doi:10.1029/2001JD900014.

Hsu, N. C., S.-C. Tsay, M. D. King, and J. R. Herman (2004), Aerosol properties over bright-reflecting source regions, *IEEE Trans. Geosci. Remote Sens.*, *42*(3), 557–569, doi:10.1109/TGRS.2004.824067.

Hsu, N. C., S.-C. Tsay, M. D. King, and J. R. Herman (2006), Deep blue retrievals of Asian aerosol properties during ACE-Asia, *IEEE Trans. Geosci. Remote Sens.*, *44*(11), 3180–3195, doi:10.1109/TGRS.2006.879540.

Hsu, N. C., M.-J. Jeong, C. Bettenhausen, A. M. Sayer, R. Hansell, C. S. Seftor, J. Huang, and S.-C. Tsay (2013), Enhanced deep blue aerosol retrieval algorithm: The second generation, *J. Geophys. Res. Atmos.*, *118*, 9296–9315, doi:10.1002/jgrd.50712.

Hyer, E. J., J. S. Reid, and J. Zhang (2011), An over-land aerosol optical depth data set for data assimilation by filtering, correction, and aggregation of MODIS Collection 5 optical depth retrievals, *Atmos. Meas. Tech.*, *4*(3), 379–408, doi:10.5194/amt-4-379-2011.

Jackson, J. M., H. Liu, I. Laszlo, S. Kondragunta, L. A. Remer, J. Huang, and H.-C. Huang (2013), Suomi-NPP VIIRS aerosol algorithms and data products, *J. Geophys. Res. Atmos.*, *118*, 12,673–12,689, doi:10.1002/2013JD020449.

Kahn, R. A., B. J. Gaitley, J. V. Martonchik, D. J. Diner, K. A. Crean, and B. Holben (2005), Multiangle Imaging Spectroradiometer (MISR) global aerosol optical depth validation based on 2 years of coincident Aerosol Robotic Network (AERONET) observations, *J. Geophys. Res.*, *110*, D10S04, doi:10.1029/2004JD004706.

Kahn, R. A., B. J. Gaitley, M. J. Garay, D. J. Diner, T. F. Eck, A. Smirnov, and B. N. Holben (2010), Multiangle Imaging SpectroRadiometer global aerosol product assessment by comparison with the Aerosol Robotic Network, *J. Geophys. Res.*, *115*, D23209, doi:10.1029/2010JD014601.

Kaufman, Y. J., D. Tanr, L. A. Remer, E. F. Vermote, and A. Chu (1997), Operational remote sensing of tropospheric aerosol over land from EOS moderate resolution imaging spectroradiometer, *J. Geophys. Res.*, *102*(96), 51–67.

Kaufman, Y. J., D. Tanré, and O. Boucher (2002), A satellite view of aerosols in the climate system, *Nature*, *419*(6903), 215–23, doi:10.1038/nature01091.

Kaufman, Y. J., O. Boucher, D. Tanré, M. Chin, L. A. Remer, and T. Takemura (2005), Aerosol anthropogenic component estimated from satellite data, *Geophys. Res. Lett.*, *32*, L17804, doi:10.1029/2005GL023125.

Levy, R. C., L. A. Remer, and O. Dubovik (2007a), Global aerosol optical properties and application to Moderate Resolution Imaging Spectroradiometer aerosol retrieval over land, *J. Geophys. Res.*, *112*, D13210, doi:10.1029/2006JD007815.

Levy, R. C., L. A. Remer, S. Mattoo, E. F. Vermote, and Y. J. Kaufman (2007b), Second-generation operational algorithm: Retrieval of aerosol properties over land from inversion of Moderate Resolution Imaging Spectroradiometer spectral reflectance, *J. Geophys. Res.*, *112*, D13211, doi:10.1029/2006JD007811.

Levy, R. C., L. A. Remer, R. G. Kleidman, S. Mattoo, C. Ichoku, R. Kahn, and T. F. Eck (2010), Global evaluation of the Collection 5 MODIS dark-target aerosol products over land, *Atmos. Chem. Phys.*, *10*(21), 10,399–10,420, doi:10.5194/acp-10-10399-2010.

Levy, R. C., S. Mattoo, L. A. Munchak, L. A. Remer, A. M. Sayer, F. Patadia, and N. C. Hsu (2013), The Collection 6 MODIS aerosol products over land and ocean, *Atmos. Meas. Tech.*, *6*(11), 2989–3034, doi:10.5194/amt-6-2989-2013.

Li, C., A. K.-H. Lau, and D. A. Chu (2005), Retrieval, validation, and application of the 1-km aerosol optical depth from MODIS measurements over Hong Kong, *IEEE Trans. Geosci. Remote Sens.*, *43*(11), 2650–2658, doi:10.1109/TGRS.2005.856627.

Li, Y., Y. Xue, X. He, and J. Guang (2011), High-resolution aerosol remote sensing retrieval over urban areas by synergetic use of HJ-1 CCD and MODIS data, *Atmos. Environ.*, *46*, 173–180, doi:10.1016/j.atmosenv.2011.10.002.

Li, Z., F. Niu, K.-H. Lee, J. Xin, W. M. Hao, B. L. Nordgren, Y. Wang, and P. Wang (2007), Validation and understanding of Moderate Resolution Imaging Spectroradiometer aerosol products (C5) using ground-based measurements from the handheld Sun photometer network in China, *J. Geophys. Res.*, *112*, D22S07, doi:10.1029/2007JD008479.

Liu, H., L. A. Remer, J. Huang, H.-C. Huang, S. Kondragunta, I. Laszlo, M. Oo, and J. M. Jackson (2014), Preliminary evaluation of S-NPP VIIRS aerosol optical thickness, *J. Geophys. Res. Atmos.*, *119*, 3942–3962, doi:10.1002/2013JD020360.

Livingston, J. M., et al. (2014), Comparison of MODIS 3 km and 10 km resolution aerosol optical depth retrievals over land with airborne sunphotometer measurements during ARCTAS summer 2008, *Atmos. Chem. Phys.*, *14*(4), 2015–2038, doi:10.5194/acp-14-2015-2014.

Munchak, L. A., R. C. Levy, S. Mattoo, L. A. Remer, B. N. Holben, J. S. Schafer, C. A. Hostetler, and R. A. Ferrare (2013), MODIS 3 km aerosol product: Applications over land in an urban/suburban region, *Atmos. Meas. Tech.*, *6*(7), 1747–1759, doi:10.5194/amt-6-1747-2013.

Nazeer, M., J. E. Nichol, and Y.-K. Yung (2014), Evaluation of atmospheric correction models and Landsat surface reflectance product in an urban coastal environment, *Int. J. Remote Sens.*, *35*(16), 6271–6291, doi:10.1080/01431161.2014.951742.

Pope, C. A., R. T. Burnett, M. J. Thun, E. E. Calle, D. Krewski, K. Ito, and G. D. Thurston (2002), Lung cancer, cardiopulmonary mortality, and long-term exposure to fine particulate air pollution, *JAMA*, *287*(9), 1132–41.

Remer, L. A., et al. (2005), The MODIS aerosol algorithm, products, and validation, *J. Atmos. Sci.*, *62*(4), 947–973, doi:10.1175/JAS3385.1.

Remer, L. A., et al. (2008), Global aerosol climatology from the MODIS satellite sensors, *J. Geophys. Res.*, *113*, D14S07, doi:10.1029/2007JD009661.

Remer, L. A., S. Mattoo, R. C. Levy, and L. A. Munchak (2013), MODIS 3 km aerosol product: Algorithm and global perspective, *Atmos. Meas. Tech.*, *6*(7), 1829–1844, doi:10.5194/amt-6-1829-2013.

Riffler, M., C. Popp, A. Hauser, F. Fontana, and S. Wunderle (2010), Validation of a modified AVHRR aerosol optical depth retrieval algorithm over Central Europe, *Atmos. Meas. Tech.*, *3*(5), 1255–1270, doi:10.5194/amt-3-1255-2010.

Sayer, A. M., N. C. Hsu, C. Bettenhausen, M.-J. Jeong, B. N. Holben, and J. Zhang (2012), Global and regional evaluation of over-land spectral aerosol optical depth retrievals from SeaWiFS, *Atmos. Meas. Tech.*, *5*(7), 1761–1778, doi:10.5194/amt-5-1761-2012.

Sayer, A. M., N. C. Hsu, C. Bettenhausen, and M.-J. Jeong (2013), Validation and uncertainty estimates for MODIS Collection 6 "Deep Blue" aerosol data, *J. Geophys. Res. Atmos.*, *118*, 7864–7872, doi:10.1002/jgrd.50600.

Shi, Y., J. Zhang, J. S. Reid, E. J. Hyer, and N. C. Hsu (2013), Critical evaluation of the MODIS Deep Blue aerosol optical depth product for data assimilation over North Africa, *Atmos. Meas. Tech.*, *6*(4), 949–969, doi:10.5194/amt-6-949-2013.

Smirnov, A., B. N. Holben, T. F. Eck, O. Dubovik, and I. Slutsker (2000), Cloud-screening and quality control algorithms for the AERONET database, *Remote Sens. Environ.*, *73*(3), 337–349, doi:10.1016/S0034-4257(00)00109-7.

Torres, O., P. K. Bhartia, J. R. Herman, A. Sinyuk, P. Ginoux, and B. Holben (2002), A long-term record of aerosol optical depth from TOMS observations and comparison to AERONET measurements, *J. Atmos. Sci.*, *59*(3), 398–413, doi:10.1175/1520-0469(2002)059<0398:ALTROA>2.0.CO;2.

Torres, O., A. Tanskanen, B. Veihelmann, C. Ahn, R. Braak, P. K. Bhartia, P. Veefkind, and P. Levelt (2007), Aerosols and surface UV products from Ozone Monitoring Instrument observations: An overview, *J. Geophys. Res.*, *112*, D24S47, doi:10.1029/2007JD008809.

Vidot, J., R. Santer, and O. Aznay (2008), Evaluation of the MERIS aerosol product over land with AERONET, *Atmos. Chem. Phys.*, *8*(24), 7603–7617, doi:10.5194/acp-8-7603-2008.

Wang, Y., Y. Xue, Y. Li, J. Guang, L. Mei, H. Xu, and J. Ai (2012), Prior knowledge-supported aerosol optical depth retrieval over land surfaces at 500 m spatial resolution with MODIS data, *Int. J. Remote Sens.*, *33*(3), 674–691, doi:10.1080/01431161.2011.577832.

Wong, M. S., K.-H. Lee, J. E. Nichol, and Z. Li (2010), Retrieval of aerosol optical thickness using MODIS 500 × 500 m^2, a study in Hong Kong and the Pearl River Delta region, *IEEE Trans. Geosci. Remote Sens.*, *48*(8), 3318–3327, doi:10.1109/TGRS.2010.2045124.

Xie, Y., Y. Zhang, X. Xiong, J. J. Qu, and H. Che (2011), Validation of MODIS aerosol optical depth product over China using CARSNET measurements, *Atmos. Environ.*, *45*(33), 5970–5978, doi:10.1016/j.atmosenv.2011.08.002.